Journal of Basics and Applied Sciences Research (JOBASR)
ISSN (print): 3026-9091, ISSN (online): 1597-9962
Volume 3(3) May 2025
DOI: https://dx.doi.org/10.4314/jobasr.v3i3.23

Semi-Analytical Approach to a Fractional-Order Model for the Dynamics and Control of Typhoid Fever

Agbata, B. C.[1*], Asante-Mensa, F.[2], Abah, E.[3], Kwabi, P. A.[2], Amoah-Mensah, J.[4], Shior, M. M.[5], Meseda, P. K.[6], Topman, N. N.[7] and Obeng-Denteh, W.[2]

[1]Department of Mathematics and Statistics, Faculty of Science, Confluence University of Science and Technology, Osara, Nigeria.
[2]Department of Mathematics, College of Science, Kwame Nkrumah University of Science and Technology, Kumasi, Ghana.
[3]Department of Mathematical Science, Faculty of Natural Sciences, Prince Abubakar Audu, University, Anyigba, Nigeria.
[4]Sunyani Technical University, Sunyani, Ghana.
[5]Department of Mathematics/ Computer Science, Benue State University, Makurdi, Nigeria.
[6]Department of Mathematics, Kogi State College of Education (Technical), Kabba, Nigeria.
[7]Department of Mathematics , Faculty of Physical Sciences, Prince University Nigeria, Nsukka Nigeria.
*Corresponding Author Email: agbatabc@custech.edu.ng

ABSTRACT

The persistent threat of typhoid fever to global public health is most severe in regions where sanitation is poor and safe drinking water is scarce. The illness, which is caused by *Salmonella Typhi*, can result in systemic infection and serious complications if not treated promptly. Populations at greater risk, particularly in low-resource environments, are especially affected due to inadequate healthcare facilities. This research presents a novel fractional-order mathematical model to assess the transmission dynamics of typhoid fever, incorporating memory effects and intricate transmission patterns that traditional integer-order models fail to capture. The study uniquely applied the Adams-Bashforth method alongside fractional-order derivatives to obtain the model's solution, offering a more accurate representation of disease progression. Sensitivity analysis showed the critical roles of treatment intervention , reducing contact rate and improved sanitation in lowering the prevalence of the disease. Furthermore, the study assesses how public health initiatives, such as enhanced water quality, hygiene education, and advancements in rapid diagnostics, influence the management of typhoid fever. Simulation results suggest that a comprehensive strategy such as effective management of contaminated agents, efficient treatment, and strengthened public health systems can greatly mitigate transmission and enhance disease management outcomes.

Keywords:
Typhoid fever,
Fractional-order model,
Adams-Bashforth method,
Sensitivity analysis,
Numerical simulations.

INTRODUCTION

Typhoid fever is a life-threatening infection caused by the bacterium *Salmonella enterica* serovar Typhi. Transmission primarily occurs through the consumption of food or water contaminated by feces from an infected or convalescent individual. Once ingested, the bacteria multiply and spread into the bloodstream, leading to systemic infection (World Health Organization, 2023). The disease is characterized by prolonged fever, fatigue, headache, nausea, abdominal pain, and constipation or diarrhea. Without appropriate antibiotic treatment, typhoid fever can result in serious complications or death. Globally, typhoid fever imposes a significant health burden, particularly in regions with inadequate access to clean water and sanitation. In 2019, it was estimated that approximately 9.2 million cases and 110,000 deaths occurred worldwide, with the highest incidence rates reported in the World Health Organization (WHO) South-East Asian, Eastern Mediterranean, and African regions (Kim *et al.*, 2023). These areas often face challenges related to infrastructure and healthcare access, exacerbating the spread and impact of the disease. Recent studies have highlighted various factors associated with an increased risk of typhoid fever. A study conducted among febrile patients identified significant associations between typhoid

fever infection and occupational status, particularly among unemployed individuals and farmers, as well as lower body mass index (BMI). The study also noted inadequate levels of knowledge, perception, and practice regarding typhoid fever prevention among the population (Tadesse *et al.*, 2024). These findings underscore the need for targeted public health interventions to address these risk factors and improve preventive measures.

The emergence of extensively drug-resistant (XDR) strains of *Salmonella Typhi* poses a growing challenge to typhoid fever management. In Pakistan, XDR typhoid strains resistant to nearly all antibiotics have been reported, complicating treatment efforts and highlighting the urgency for improved water and sanitation infrastructure, as well as prudent antibiotic use (The Guardian, 2024). In response to the escalating threat, several countries have introduced typhoid conjugate vaccines (TCVs) into their national immunization programs since 2018, aiming to reduce the incidence of the disease and combat the spread of resistant strains (Kim *et al.*, 2023). Fractional-order mathematical modeling has emerged as a powerful tool in understanding the dynamics of infectious diseases. By extending traditional integer-order models to include derivatives of non-integer order, these models effectively incorporate memory effects and hereditary properties inherent in biological systems, leading to more accurate representations of disease progression (Kumar et al., 2024). For instance, a fractional-order SEIQRDP model was developed to simulate COVID-19 dynamics, demonstrating improved predictive capabilities over classical models (Patel *et al.*, 2023). Similarly, a fractional-order model for measles infection utilizing the Caputo derivative provided a more comprehensive analysis of the disease's transmission dynamics (Tadesse *et al.*, 2024).

Sharma et al. (2024) developed a fractional-order SEI1I2I3QCR model incorporating awareness and delay differential equations to simulate the progression of the COVID-19 pandemic. The study demonstrated that fractional-order models provide more accurate predictions than classical integer-order models by accounting for memory effects in disease transmission. Ali *et al.* (2024) proposed a fractional-order mathematical model to analyze tuberculosis (TB) transmission, incorporating the impact of vaccination. Their research highlighted how fractional derivatives enhance the model's accuracy in capturing TB dynamics, particularly in scenarios involving long incubation periods and vaccine efficacy. Tadesse et al. (2024) investigated the co-infection dynamics of COVID-19 and malaria using a fractional-order model with Caputo-type derivatives. The study analyzed the stability of the model and demonstrated the effectiveness of fractional calculus in simulating co-infection scenarios, improving predictions of disease outbreaks. Gomez *et al.* (2023) developed a fractional-order SEIR (Susceptible-Exposed-Infected-Recovered) model to analyze COVID-19 transmission in Buenos Aires. The study found that incorporating memory effects improved model accuracy in predicting case trends and evaluating the impact of lockdown measures.

MATERIALS AND METHODS

Preliminary

Definition 1: Let $f \in \Lambda^{\infty}(R)$, then the right and left Function's Caputo fractional derivative

$$ {}^{a}D_{t}^{\beta} f(t) = \left(t^{0}D_{t}^{-(c-\beta)} \left(\frac{d}{dt} \right)^{c} f(t) \right) $$

$$ {}^{a}D_{t}^{\beta} f(t) = \frac{1}{\Gamma(c-\beta)} \int_{0}^{t} \left((t-\lambda)^{c-\beta-1} f^{c}(\lambda) \right) d\lambda \quad (1) $$

In a similar vein

$$ {}_{T}^{a}D_{t}^{\beta} f(t) = \left({}_{t}D_{T}^{-(-\beta)} \left(\frac{-d}{dt} \right)^{a} f(t) \right) $$

$$ {}_{T}^{a}D_{T}^{\beta} f(t) = \frac{(-1)^{b}}{\Gamma(c-\beta)} \int_{t}^{T} \left((\lambda-t)^{c-\beta-1} f^{c}(\lambda) \right) d\lambda $$

Definition 2: The Mittag-Leffler function in generalized form $E_{\xi,\alpha}(x)$ for $x \in R$ is given by

$$ E_{\xi,\alpha}(x) = \sum_{c=0}^{\infty} \frac{x^{c}}{\Gamma(\xi c + \alpha)}, \xi, \alpha > 0 \quad (2) $$

$$ E_{\xi,\alpha}(x) = x E_{\xi,\xi+\alpha(x)} + \frac{1}{\Gamma(\alpha)} \quad (3) $$

$$ t^{\alpha-1} E_{\xi,\alpha}\left(\pm \psi t^{\xi} \right) $$

Taking the Laplace transform, yilds equation (4)

$$ L\left[t^{\alpha-1} E_{\xi,\alpha\left(\pm\psi t^{\xi}\right)} \right] = \frac{S^{\xi-\alpha}}{S^{\xi} \pm \psi} \quad (4) $$

Proposition 1.1 Let $f \in \Lambda^{\infty}(R) \cap d(R)$ and $\xi \in R$, $c-1 < \xi < c$, Consequently, the following requirements are met:

1. $${}_{t_0}^{a}D_t^{\beta} I^{\beta} f(t) = f(t)$$

2. $$I_{t_0}^{\beta} D_t^{\beta} f(t) = f(t) - \sum_{k=0}^{c-k} \frac{t^k}{k!} f^k(t_o).$$

Model Formulation

In this segment, a deterministic compartmental model for the transmission dynamics of typhoid fever is developed. The total human population $N(t)$, is subdivide into five (5) epidemiological classes of susceptible humans S, exposed humans to diarrhea infection E, infected humans I,, treatment class of typhoid fever T, and recovered individuals R. Let Λ denotes recruitment rate of individuals into the susceptible compartment, where β is the effective contact rate with the probability of infection per contact with infected human. The population of exposed human is decreased by infection rate α and treatment rate of exposed humans θ, where ϕ is the treatment rate of infectious individuals and each of the compartment is decreased by the natural death rate μ and σ denotes diseased induced rate. Every treated human recovers at the ψ rate, where immunity loss occurs recovered individuals become susceptible at the ω rate. Based on the schematic diagram in figure 1 and the model description, we have the following differential equations

$$\begin{aligned}
\frac{dS}{dt} &= \Lambda + \omega R - \frac{\beta SI}{N} - \mu S,\\
\frac{dE}{dt} &= \frac{\beta SI}{N} - (\alpha + \theta + \mu)E,\\
\frac{dI}{dt} &= \alpha E - (\sigma + \phi + \mu)I,\\
\frac{dT}{dt} &= \theta E + \phi I - (\psi + \mu)T,\\
\frac{dR}{dt} &= \psi T - (\omega + \mu)R.
\end{aligned} \tag{5}$$

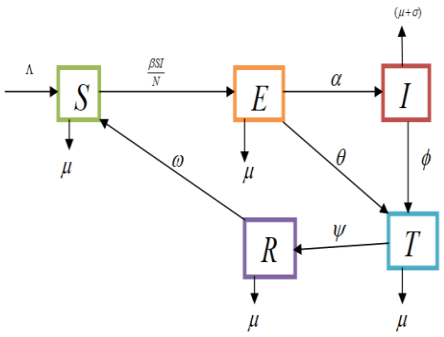

Figure 1. Schematic diagram for the typhoid fever model (1)

Fractional typhoid fever mathematical model

In this section, the integer-order model of typhoid fever from Equation (5) transformed into the Caputo fractional derivative operator (Abah, *et al*, 2025). This fractional model introduces greater flexibility compared to the classical model, as it allows the system's behavior to adapt and exhibit a range of dynamic responses. The fractional modeling approach for Diphtheria is thus formulated as follows:

$$\begin{aligned}
{}^{a}D_t^{\beta} S &= \Lambda + \omega R - \frac{\beta SI}{N} - \mu S,\\
{}^{a}D_t^{\beta} E &= \frac{\beta SI}{N} - B_1 E,\\
{}^{a}D_t^{\beta} I &= \alpha E - B_2 I,\\
{}^{a}D_t^{\beta} T &= \theta E + \phi I - B_3 T,\\
{}^{a}D_t^{\beta} R &= \psi T - B_4 R.
\end{aligned} \tag{6}$$

Where

$$B_1 = (\alpha + \theta + \mu), B_2 = (\sigma + \phi + \mu), B_3 = (\psi + \mu),$$
$$B_4 = (\omega + \mu).$$

Assuming suitable initial conditions:

$$S(0) = S_0, E(0) = E_0, I(0) = I_0, T(0) = T_0,$$
$$R(0) = R_0. \tag{7}$$

Model Analysis

Positivity of solution

Considering the non-negativity of the initial values.

$$\lim Sup.N(t) \le \frac{\Lambda}{\mu},$$

Secondly, If $\lim Sup.N_0(t) \le \frac{\Lambda}{\mu}$,

The feasible region of the model is given by:

$$\Psi = \left\{ (S,E,I,T,R) \subset R_+^5 : S + E + I + T + R \le \frac{\Lambda}{\mu}, \right\}$$
$$\Psi \subset R_+^5,$$

Hence Ψ is positively invariant.

If S, E, I, T, R are non-negative, so that the solution of model (6) will also be non-negative for $t > 0$.

By taking the first equation from Eq. (6), we obtain:

$${}^{a}D_t^{\beta} S = \Lambda + \omega R - \frac{\beta SI}{N} - \mu S,$$

$${}^{a}D_t^{\beta} S + \frac{\beta SI}{N} + \mu S = \Lambda + \omega R$$

But $\Lambda + \omega R \geq 0,$
then

$$^{a}D_{t}^{\beta}S + \frac{\beta SI}{N} + \mu S \geq 0$$

$$L\left[{}^{a}D_{t}^{\beta}S\right] + L\left[\frac{\beta SI}{N} + \mu S\right] \geq 0$$

$$S^{\beta}S(s) - S^{\beta-1}S(0) + \frac{\beta SI}{N} + \mu S(s) \geq 0,$$

$$S(t) \geq \frac{S^{\beta-1}}{\left(S^{\beta} + \frac{\beta SI}{N} + \mu S\right)} S_0.$$

By applying the inverse Laplace transform, we have

$$S(t) \geq E_{\beta,1}\left(-\left(\frac{\beta I}{N} + \mu\right)\right)S_0 \qquad (8)$$

Since the term on the right-hand side of equation (8) is positive, we deduce that $S \geq 0$ for $t \geq 0$. Also, since $E \geq 0$, $I \geq 0, T \geq 0, R \geq 0,$ are positive , the solutions remain within the real number set R_{+}^{5} for all $t \geq 0$ with positive initial conditions.

Boundedness of solution of the fractional-order model

The total number of people in our model is given by:

$N(t) = S(t) + E(t) + I(t) + R(t).$

Thus, by using our fractional model (6), we can now:

$$^{a}D_{t}^{\beta}N(t) = {}^{a}D_{t}^{\beta}S(t) + {}^{a}D_{t}^{\beta}E(t) + {}^{a}D_{t}^{\beta}I(t) + {}^{a}D_{t}^{\beta}R(t)$$

$$^{a}D_{t}^{\beta}N(t) = \Lambda - \mu N(t) \qquad (9)$$

Taking the Laplace transform of equation (9), we have:

$$L\left[{}^{a}D_{t}^{\beta}N(t)\right] \leq L\left[\Lambda - \mu N(t)\right],$$

$$S^{\beta}N(S) - S^{\beta-1}N(0) + \mu N(S) \leq \tfrac{\Lambda}{S},$$

$$N(\mathrm{s}) \leq \frac{S^{\beta-1}}{\left(S^{\beta} + \mu\right)}N(0) + \frac{\Lambda}{S\left(S^{\beta} + \mu\right)} \qquad (10)$$

Taking the inverse Laplace transform of equation (10) yields:

$$N(t) \leq E_{\beta,1}\left(-\mu t^{\beta}\right)N(0) + \Lambda E_{\beta,\beta+1}\left(-\mu t^{\beta}\right) \qquad (11)$$

At $t \to \infty$, the limit of equation (11) becomes

$$\lim_{t\to\infty} SupN(t) = \frac{\Lambda}{\mu}.$$

This means that, if $N \leq \frac{\Lambda}{\mu}$ then $N(t) \leq \frac{\Lambda}{\mu}$ which implies that, $N(t)$ is bounded.

We can therefore conclude that, from an epidemiological perspective, this region Ψ is both pe and well-posed.

Existence and uniqueness of our model solution

Let T be a real nonnegative number, given that $X = [0, T]$. The collection of every continuous function defined on Z is denoted by $N_{e}^{0}Z$ with norm as

$$\|P\| = \sup\left\{\left|P(t)\right| t, \in Z\right\}.$$

Taking into account model (6) with the starting conditions given in (7), which is modeled as an initial value problem (IVP) in (12)

$$^{a}D_{t}^{\beta}P(t) = P\left(t, K(x)\right), 0 < t < T < \infty,$$

$$P(0) = P_0. \qquad (12)$$

Where $P(t) = \left(S(t), E(t), I(t), T(t), R(t)\right)$ symbolizes the classes, and K is a continuous function with the following definition;

$$K_1\left(t, P(t)\right) = \begin{pmatrix} K_1\left(t, S(t)\right) \\ K_2\left(t, E(t)\right) \\ K_3\left(t, I(t)\right) \\ K_4\left(t, T(t)\right) \\ K_5\left(t, R(t)\right) \end{pmatrix}$$

$$= \begin{pmatrix} \Lambda + \omega R - \frac{\beta SI}{N} - \mu S, \\ \frac{\beta SI}{N} - (\alpha + \theta + \mu)E, \\ \alpha E - (\sigma + \phi + \mu)I, \\ \theta E + \phi I - (\psi + \mu)T, \\ \psi T - (\omega + \mu)R \end{pmatrix} \qquad (13)$$

Using proposition, we have that,

$$S(t)=S_0+I_t^{\beta}\left[\Lambda+\omega R-\frac{\beta SI}{N}-\mu S\right],$$
$$E(t)=E_0+I_t^{\beta}\left[\frac{\beta SI}{N}-(\alpha+\theta+\mu)E\right],$$
$$I(t)=I_0+I_t^{\beta}\left[\alpha E-(\sigma+\phi+\mu)I\right],$$
$$T(t)=T_0+I_t^{\beta}\left[\theta E+\phi I-(\psi+\mu)T\right],$$
$$R(t)=R_0+I_t^{\beta}\left[\psi T-(\omega+\mu)R\right]. \quad (14)$$

The Picard iterations of equation (14) are obtained below:

$$S(t)=S_0+\frac{1}{\Gamma(\beta)}\int_0^t(t-\lambda)^{\beta-1}K_1\left(\lambda,S_{n-1}(\lambda)\right)d\lambda,$$
$$E(t)=E_0+\frac{1}{\Gamma(\beta)}\int_0^t(t-\lambda)^{\beta-1}K_2\left(\lambda,E_{n-1}(\lambda)\right)d\lambda,$$
$$I(t)=I_0+\frac{1}{\Gamma(\beta)}\int_0^t(t-\lambda)^{\beta-1}K_3\left(\lambda,I_{n-1}(\lambda)\right)d\lambda,$$
$$T(t)=T_0+\frac{1}{\Gamma(\beta)}\int_0^t(t-\lambda)^{\beta-1}K_4\left(\lambda,I_{n-1}(\lambda)\right)d\lambda,$$
$$R(t)=R_0+\frac{1}{\Gamma(\beta)}\int_0^t(t-\lambda)^{\beta-1}K_5\left(\lambda,R_{n-1}(\lambda)\right)d\lambda. \quad (15)$$

Applying the initial value problem in equation (12) yields;

$$P(t)=P(0)+\frac{1}{\Gamma(\beta)}\int_0^t(t-\lambda)^{\beta-1}K\left(\lambda,K(\lambda)\right)\mathrm{d}\lambda. \quad (16)$$

Lemma 1. The vector $K\left(t,P(t)\right)$ satisfies the Lipschitz requirement as stated in Eq. (13) on a set $[0,T]\times R_+^5$ with the Lipchitz constant given as;

$$\Omega=\max\begin{pmatrix}(I^*+\mu),(\mu+\alpha+\theta),(\mu+\sigma+\phi),\\(\mu+\psi),(\mu+\omega).\end{pmatrix}$$

Proof

$$\left\|K_1(t,S)-K_1(t,S)\right\|$$
$$\left\|\begin{matrix}\Lambda+\omega R-\frac{\beta SI}{N}-\mu S\\-\left(\Lambda-\frac{\beta I}{N}+\mu\right)S+\omega R\end{matrix}\right\|$$
$$\left\|-\left(\frac{\beta I}{N}\right)(S-S_1)+\mu(S-S_1)\right\|$$
$$\le(\beta^*)\left\|(S-S_1)\right\|+\left\|\mu(S-S_1)\right\|$$

$$\therefore\left\|K_1(t,S)-K_1(t,S_1)\right\|\le(\beta^*+\mu)\left\|S-S_1\right\|.$$

Likewise, we discovered the following:

$$\left\|K_2(t,E)-K_2(t,E_1)\right\|\le(\alpha+\theta+\mu)\left\|E-E_1\right\|,$$
$$\left\|K_3(t,I)-K_3(t,I_1)\right\|\le(\sigma+\phi+\mu)\left\|I-I_1\right\|,$$
$$\left\|K_4(t,T)-K_4(t,T_1)\right\|\le(\psi+\mu)\left\|T-T_1\right\|,$$
$$\left\|K_5(t,R)-K_5(t,R_1)\right\|\le(\omega+\mu)\left\|R-R_1\right\|.$$

Where we obtained

$$\left\|K\left(t,P(t)\right)-K\left(t,P_2(t)\right)\right\|\le\Omega\left\|P_1-P_2\right\|.$$
$$\Omega=\max\begin{pmatrix}(I^*+\mu),(\mu+\alpha+\theta),(\mu+\sigma+\phi),\\(\mu+\psi),(\mu+\omega).\end{pmatrix} \quad (18)$$

Lemma 2: There exist solutions to the initially value problems (6), (7) in Eq. (18).

$K(t)\in L_c^0(F).$

We examine the solution using fixed point theory and Picard-Lindel of $K(t)=S\left(P(t)\right)$, When the Picard operator, represented as S, is defined as;

$S:L_C^0\left(F,R_+^*\right)\to L_C^0\left(F,R_+^5\right).$

Therefore,

$$S\left(K(t)\right)=K(0)+\frac{1}{\Gamma(\beta)}\int_0^t(t-\lambda)^{\beta-1}P\left(\lambda,P(\lambda)\right)\mathrm{d}\lambda$$

$$\left\|S\left(P_1(t)\right)-S\left(P_2(t)\right)\right\|$$

$$\left\| \frac{1}{\Gamma(\beta)} \int_0^t (t-\lambda)^{\beta-1} \left[K\left(\lambda, K_1(\lambda)\right) - K\left(\lambda, P_2(\lambda)\right) d\lambda \right] \right\|$$

$$\leq \frac{1}{\Gamma(\beta)} \int_0^t (t-\lambda)^{\beta-1} \left\| K\left(\lambda, P_1(\lambda)\right) - K\left(\lambda, P_2(\lambda)\right) d\lambda \right\|$$

$$\leq \frac{\Omega}{\Gamma(\beta)} \int_0^t (t-\lambda)^{\beta-1} \left\| P_1 - P_2 \right\| d\lambda$$

$$\therefore \left\| S\left(P_1(t)\right) - S\left(P_2(t)\right) \right\| \leq \frac{\Omega}{\Gamma(\beta+1)S}$$

When $\frac{\Omega}{\Gamma(\beta+1)} S \leq 1$ the solutions to Equations (6) and (7) are unique since the Picard operator produces a contradiction.

The basic reproduction number (R_0) and model equilibrium points:

The disease-free equilibrium point of model (5) is given below:

$$Z_0 = \left(S^*, E^*, I^*, T^*, R^*\right) = \left(\frac{\Lambda}{\mu}, 0, 0, 0, 0\right)$$

Following the approach in (VendenDriessche and Watmough, 2002; Diethelm, 199). We obtain the basic production number as follows

$$let\ u = (E, I, T, R)$$

So that $\frac{du}{dt} = F - V.$

Where;

$$F = \begin{bmatrix} \beta & 0 & 0 \\ 0 & 0 & 0 \\ 0 & 0 & 0 \end{bmatrix},\ V = \begin{bmatrix} K_1 & -\theta & 0 \\ -\alpha & K_2 & -\phi \\ 0 & -\psi & K_3 \end{bmatrix},$$

$$FV^{-1} = \begin{bmatrix} \frac{\beta\alpha K_3}{K_1K_2K_3 + \phi\alpha\psi} & \frac{\beta\phi K_1}{K_1K_2K_3 + \phi\alpha\psi} & -\frac{\beta\phi\psi}{K_1K_2K_3 + \phi\alpha\psi} \\ 0 & 0 & 0 \\ 0 & 0 & 0 \end{bmatrix}.$$

Thus, the basic reproduction number for the typhoid model is given as:

$$R_0^{Ty} = \frac{\beta\alpha K_3}{K_1K_2K_3 + \phi\alpha\psi} \qquad (20)$$

Where

$K_1 = \mu, \quad K_2 = \alpha + \theta + \mu, \quad K_3 = \sigma + \phi + \mu.$

Mathematically, the basic reproduction number is computed as $R_0 = \rho\left(FV^{-1}\right)$ where ρ is the dominant Eigen value of the system $\left(FV^{-1}\right)$. Where R_0^H is the basic reproduction number associated with the individuals in the population (Bolaji *et al.*, 2024)

Endemic equilibrium point

The endemic equilibrium point is the state where the disease persists in the population, there is a positive stable state known as the endemic equilibrium point. The variables in the model are not zero at this equilibrium point.

$\left(S^* \neq 0, E^* \neq 0,\ I^* \neq 0, T^* \neq 0, \text{and } R^* \neq 0\right)$

The model equations are solved in terms of the force of infection linked with human populations in order to examine the endemic equilibrium point. Based on the fractional Tuberculosis model (6), the endemic equilibrium state is symbolized as follows:

$$\zeta = (S^*, E^*, I^*, T^*, R^*)$$

Defined as;

$$S^{**} = \frac{\Lambda K_3 K_2}{K_1K_2K_3 + \phi\alpha\psi},\ E^{**} = \frac{\beta S^{**} I^{**}}{K_2},$$

$$I^{**} = \frac{\alpha E^{**}}{K_3},\ T^{**} = \frac{\theta E^{**} + \phi I^{**}}{\psi + \mu},\ R^{**} = \frac{\psi T^{**}}{\omega + \mu}.$$

Substituting these equilibrium values into the force of infection:

$$\lambda^{**} = \frac{\beta I^{**}}{N}.$$

We obtained:

$$(A\lambda^{**} + B)\lambda^{**} = 0,$$

where:

$$A = \beta\alpha K_3,$$

$$B = K_1K_2K_3 + \phi\alpha\psi\left(1 - R_0^{Ty}\right).$$

At the endemic equilibrium point, $\lambda^{**} \neq 0$, thus:

This implies:

$$A\lambda^{**} + B = 0.$$

$$\Rightarrow R_0^{Ty} - 1 > 0 \quad \text{and} \quad R_0^{Ty} > 1.$$

Consequently, the typhoid model endemic equilibrium is stable whenever $R_0^{Ty} > 1$.

Sensitivity Analysis of the typhoid Model

Sensitivity analysis is used to identify the factors that encourage both the containment and spread of typhoid within a population. For any parameter p, the sensitivity index of the reproduction number of the typhoid model is given by:

$$\Im_p^{R_0} = \frac{\partial R_0}{\partial p} \times \frac{p}{R_0}$$

The basic reproduction number for the typhoid model is expressed as:

$$R_0^{Ty} = \frac{\beta\alpha K_3}{K_1K_2K_3 + \phi\alpha\psi},$$

where:

$$K_1 = \mu, \quad K_2 = \alpha + \theta + \mu, \quad K_3 = \sigma + \phi + \mu.$$

Using the sensitivity formula, the sensitivity indices for the parameters are computed as follows:

Transmission Rate (β):

$$\Im_\beta^{R_0} = \frac{\partial R_0}{\partial \beta} \times \frac{\beta}{R_0} = 1$$

Progression Rate (α):

$$\Im_\alpha^{R_0} = \frac{\partial R_0}{\partial \alpha} \times \frac{\alpha}{R_0}$$

Differentiating R_0^{Ty} with respect to α yields:

$$\frac{\partial R_0}{\partial \alpha} = \frac{\beta K_3}{K_1K_2K_3 + \phi\alpha\psi} - \frac{\beta\alpha K_3\phi\psi}{(K_1K_2K_3 + \phi\alpha\psi)^2}.$$

Substituting values and simplifying:

$$\Im_\alpha^{R_0} = 0.728.$$

$$\Im_\theta^{R_0} = \frac{\partial R_0}{\partial \theta} \times \frac{\theta}{R_0}.$$

Differentiating R_0^{Ty} with respect to θ through K_2 yields:

$$\frac{\partial R_0}{\partial \theta} = -\frac{\beta\alpha K_3K_1}{(K_1K_2K_3 + \phi\alpha\psi)^2}.$$

Substituting values and simplifying:

$$\Im_\theta^{R_0} = -0.135.$$

$$\Im_\mu^{R_0} = \frac{\partial R_0}{\partial \mu} \times \frac{\mu}{R_0}.$$

The contributions of μ arise through K_1, K_2, and K_3.

After computation:

$$\Im_\mu^{R_0} = -0.093.$$

Treatment Rate (σ):

$$\Im_\sigma^{R_0} = \frac{\partial R_0}{\partial \sigma} \times \frac{\sigma}{R_0}.$$

Since σ is part of K_3:

$$\frac{\partial R_0}{\partial \sigma} = \frac{\beta\alpha}{K_1K_2K_3 + \phi\alpha\psi}.$$

Substituting values and simplifying:

$$\Im_\sigma^{R_0} = 0.094.$$

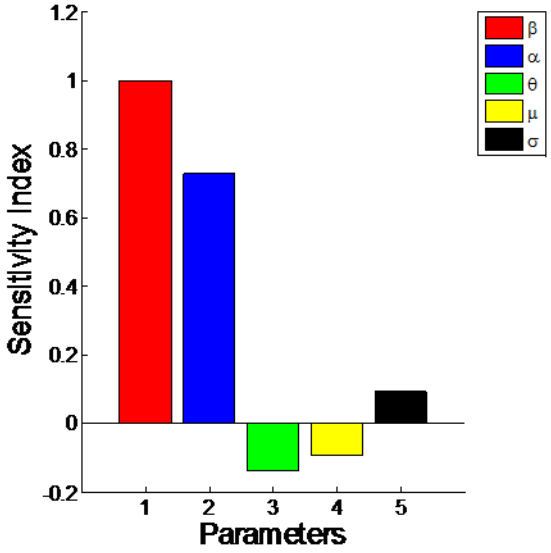

Figure 2. Bar chat of Typhoid Fever Sensitivity Indices

The sensitivity bar chart above provides a comprehensive analysis of the key parameters influencing the transmission dynamics of typhoid fever. Parameters with **positive sensitivity indices** indicate factors that contribute to an increase in disease transmission. Notably, the **contact rate** and **infectious rate** exhibit positive sensitivity indices, demonstrating that higher values of these parameters lead to a greater spread of typhoid fever. This implies that any measures aimed at reducing contact rate such as improved hygiene practices, social distancing in outbreak scenarios, and public awareness campaigns can play a crucial role in mitigating disease transmission. Similarly, controlling the infectious rate through early diagnosis, prompt treatment, and isolation of infected individuals can significantly curb the spread of typhoid fever (Agbata et al., 2024,). Conversely, parameters with **negative sensitivity indices** highlight factors that contribute to disease reduction. One such parameter is the **treatment rate**, which shows a strong negative sensitivity index, indicating that an increase in timely and effective medical interventions significantly lowers the prevalence of typhoid fever. This underscores the

importance of **enhancing treatment accessibility**, particularly in low-resource settings where inadequate healthcare facilities contribute to prolonged infection and continued transmission (Odeh *et al., 2024)* Strengthening healthcare infrastructure, ensuring the availability of antibiotics, and improving patient adherence to prescribed treatment regimens are critical steps in reducing disease burden.

Implementation of fractional Adams–Bashforth–Moulton method

The approach proposed by Baskonus *et al.* (2015) and Diethelm *et al.* (1999) serves as the foundation for this study. In this work, we apply their methodology to develop an approximate solution for the fractional-order tuberculosis model described in Equation (6). To achieve this, we employ the fractional Adams–Bashforth method, a numerical technique well-suited for solving fractional differential equations. This method effectively captures the memory effects and complex dynamics inherent in fractional-order systems, offering a more accurate representation of the disease transmission process. Consequently, the fractional-order model presented in Equation (6) is reformulated as follows:

$$ {}^{a}D_t^{\beta} X(t) = Z\left(t, Q(t)\right),\ 0 < t < \psi,$$

$$ Q^{(n)}(0) = Q_0^{(n)},\ n = 1, 0, ..., Q, Q = [\beta]. \quad (24)$$

Where $Q = \left(S^*, E^*, I^*, T^*, R^*\right) \in R_+^5$ and $K\left(t, Z(t)\right)$ is a real valued function that is continuous.

Therefore, the following representation of Eq. (24) can be made using the idea of a fractional integral:

$$ Q(t) = \sum_{n=0}^{q-1} Q_0^{(n)} \frac{t^n}{n!} + \frac{1}{\Gamma(\beta)} \int_0^t (t-q)^{\beta-1} K\left(q, Q(q)\right) dq \quad (25)$$

Using the method described by [7], we let the step size $d = \frac{\psi}{N},\ N \in \mathrm{N}$ with a grid that is uniform on $[0, \psi]$.

Where $t_c = cr,\ c = 0, 1, 1, ...N.$ Therefore, the fractional order model of Typhoid model presented in (6) can be approximated as:

$$ S_{k+1}(t) = S_0 + \frac{d^{\beta}}{\Gamma(\beta+2)} \left\{ \Lambda + \omega R^n - \left(\beta I^n\right) \frac{S^n}{N} - \mu S^n \right\} + \frac{d^{\beta}}{\Gamma(\beta+2)} \sum_{q=0}^{k} dq, k+1 \left\{ \Lambda + \omega R_q - \left(\beta I_q\right) \frac{S_q}{N} - \mu S_q \right\},$$

$$ E_{k+1}(t) = E_0 + \frac{d^{\beta}}{\Gamma(\beta+2)} \left\{ \left(\beta I^n\right) \frac{S^n}{N} - (\alpha + \theta + \mu) E^n \right\} + \frac{d^{\beta}}{\Gamma(\beta+2)} \sum_{q=0}^{k} dq, k+1 \left\{ \left(\beta I_q\right) \frac{S_q}{N} - (\alpha + \theta + \mu) E_q \right\},$$

$$ I_{k+1}(t) = I_0 + \frac{d^{\beta}}{\Gamma(\beta+2)} \left\{ \alpha E^n - (\sigma + \phi + \mu) I^n \right\} + \frac{d^{\beta}}{\Gamma(\beta+2)} \sum_{q=0}^{k} dq, k+1 \left\{ \alpha E_q - (\sigma + \phi + \mu) I_q \right\},$$

$$ T_{k+1}(t) = T_0 + \frac{d^{\beta}}{\Gamma(\beta+2)} \left\{ \theta E^n + \phi I^n - (\psi + \mu) T^n \right\} + \frac{d^{\beta}}{\Gamma(\beta+2)} \sum_{q=0}^{k} dq, k+1 \left\{ \theta E_q + \phi I_q - (\psi + \mu) T_q \right\},$$

$$ R_{k+1}(t) = R_0 + \frac{d^{\beta}}{\Gamma(\beta+2)} \left\{ \psi T^n - (\omega + \mu) R^n \right\} + \frac{d^{\beta}}{\Gamma(\beta+2)} \sum_{q=0}^{k} dq, k+1 \left\{ \psi T_q - (\omega + \mu) R_q \right\}, \quad (26)$$

where

$$ S_{(k+1)}(t) = \frac{1}{\Gamma(\beta)} \sum_{q=0}^{k} e_q k+1 \left\{ \Lambda + \omega R_q - \left(\beta I_q\right) \frac{S_q}{N} - \mu S_q \right\},$$

$$ E_{(k+1)}(t) = \frac{1}{\Gamma(\beta)} \sum_{q=0}^{k} e_q k+1 \left\{ \left(\beta I_q\right) \frac{S_q}{N} - (\alpha + \theta + \mu) E_q \right\},$$

$$ I_{(k+1)}(t) = \frac{1}{\Gamma(\beta)} \sum_{q=0}^{k} e_q k+1 \left\{ \alpha E_q - (\sigma + \phi + \mu) I_q \right\},$$

$$ T_{(k+1)}(t) = \frac{1}{\Gamma(\beta)} \sum_{q=0}^{k} e_q k+1 \left\{ \theta E_q + \phi I_q - (\psi + \mu) T_q \right\},$$

$$R_{(k+1)}(t)=\frac{1}{\Gamma(\beta)}\sum_{q=0}^{k}e_q k+1\left\{\psi T_q-(\omega+\mu)R_q\right\}. \tag{27}$$

Equations (25) and (26) provided us with;

$$dq,_{K+1}=K^{\beta+1}-(k-\beta)(k+\beta)^{\beta},\ q=0$$

$$(k-q+2)^{\beta+1}+(k-\beta)^{\beta+1}-2(k-q+1)^{\beta+1},$$

$$1\le q\le k$$

$$1, q=k+1$$

And

$$e_{q,k+1}=\frac{d^{\beta}}{\beta}\left[(k-q+1)^{\beta}(k-q)^{\beta}\right],\ 0\le q\le k.$$

RESULTS AND DISCUSSION

Numerical Simulation

The numerical simulation of our model equations is carried out using MATLAB to illustrate the real-world dynamics of the system through graphical representations (Agbata et al., 2024). We examined the impact of various parameters on disease transmission and evaluate the effectiveness of different intervention strategies. The simulation offers valuable insights into key trends, including the temporal changes in susceptible, exposed, infected, and recovered populations.

Table 1. Parameter values used in the model

Parameter	Value	Source
Λ	10726.4451	Omowumi *et al* , 2024
β	0.00000001	Omowumi *et al*, 2024
μ	0.040	Omowumi *et al*, 2024
σ	0.005	Bolarinwa *et al* , 2024
α	0.05	Acheneje *et al*, 2024
θ	0.100	Omowumi *et al*, 2024
ϕ	0.01	Agbata *et al*, 2023
ω	0.01	Odeh *et al*, 2024

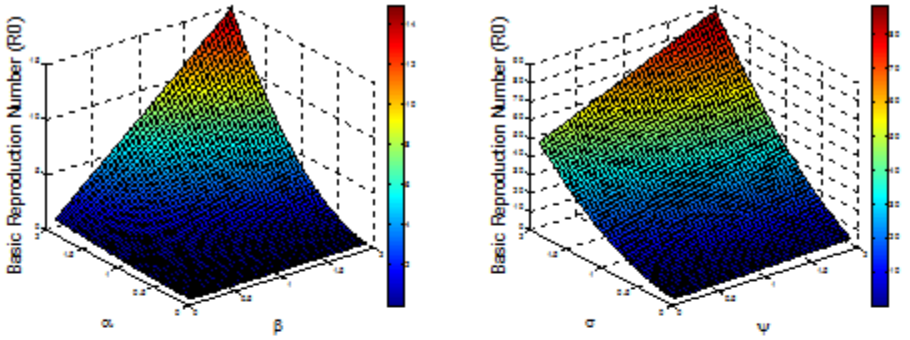

(b) Impact of α and β on R_0^T (a) Impact of σ and ψ on R_0^T

Figure 3: surface plot of the basic

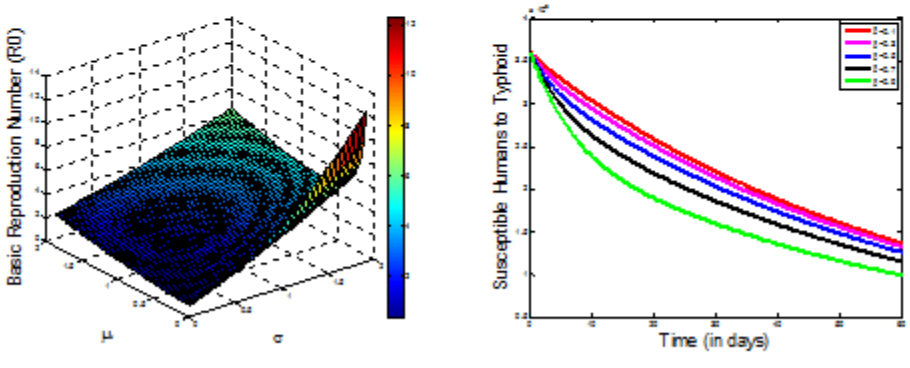

(a) Impact of μ and σ on R_0^T (b) Simulation of Susceptible Humans to Typhoid

Figure 4: surface plot and Effect of β on $S_H(t)$

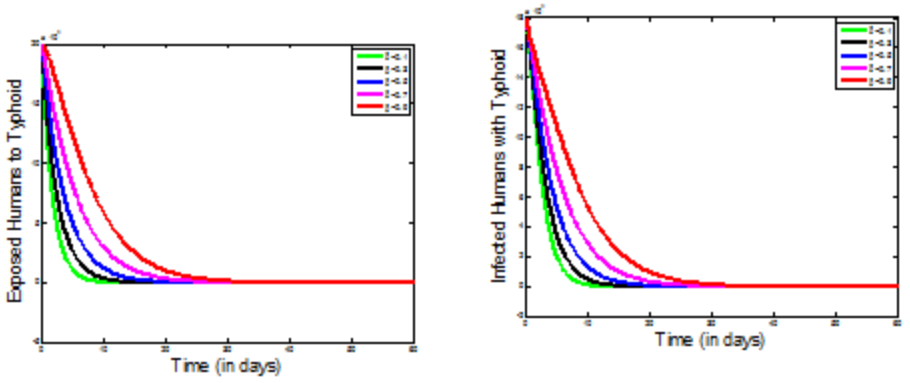

(a) **Simulation of Exposed Humans to Typhoid** (b) **Simulation of Infected Humans to Typhoid**

Figure: 5 Effect of β on $E(t)$ and $I(t)$

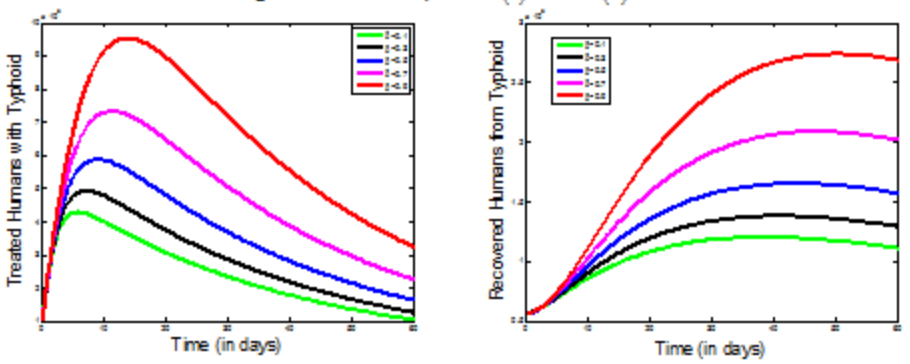

(a) **Simulation of Treated Humans to Typhoid** (b) **Simulation of Recovered Humans to Typhoid**

Figure: 6 Effect of β on $T(t)$ and $R(t)$

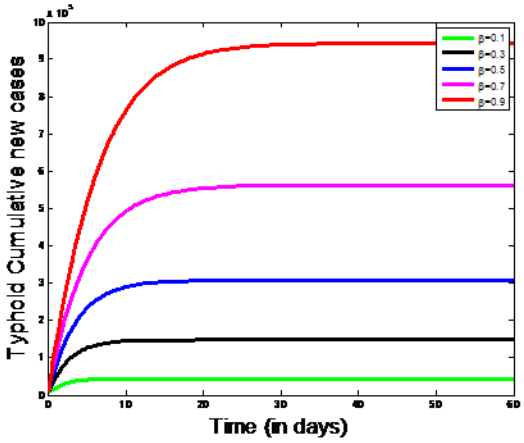

Figure: 7 Effect of β on the cumulative new cases of Typhoid

Figure 3(a) reveals that an increase in the parameters α and β indicating the contact rate and the progression rate of exposure to typhoid-infected persons, respectively, which, as evidenced by a basic reproduction number R_0^T above one (1), raises the incidence of typhoid in human populations. The surface plot in Figure 3(b) shows the effects of different between σ and ψ, showing the disease-induced mortality rate of typhoid-affected individuals and the recovery rate of typhoid-affected humans relative to the basic reproduction number R_0^T of the population, It was shown that when these parameters are increased, the value of R_0^T peaks and falls below one. This suggests that lowering the rate at which individuals are exposed to typhoid-causing chemicals and implementing policies that promote appropriate treatment may eventually lessen the incidence of typhoid among humans. Figure 4(a) shows the impact of varying σ (Disease induced death rate of infected typhoid) and μ (Natural death rate of humans) on the basic reproduction number R_0^m. As demonstrated by their impact on the basic reproduction number, which can go over one (1), factors σ and μ have the potential to exacerbate the occurrence of typhoid if proper precautions are not taken. Figure 4(b) illustrates how changes in the fractional-order derivative β impact the susceptible human population

over time. The graph shows that as β increases, there are fewer people who are susceptible. This decrease occurs because fewer people are at risk of acquiring the illness as a result of the treatment plan. Figure 5(a) demonstrates that the exposed population decreases rapidly as infection rates rise. This shows that even though the overall exposed population is shrinking due to higher infectiousness, there is still a steady influx of individuals transitioning from the susceptible group to the exposed group. In Figure 5(b), the trends of the infected human population are depicted over time. Initially, the number of infected individuals grows due to the flow of people from the exposed group. However, after a certain point, this number starts to decline, thanks to treatment interventions. This highlights the effectiveness of treatment strategies in ultimately reducing the typhoid burden within the population.

Figure 6(a**)** shows how the number of people undergoing treatment has changed over time. As individuals move from the infected group to the receiving group, the treated population initially grows. However, when effective medical treatments lead to typhoid recovery, this number steadily declines over time. Figure 6(b) demonstrates an increase in the population that has recovered as treatment rates climb. This demonstrates how well healthcare tactics work to fight the illness. However, as those who recover from typhoid may re-enter the cycle of disease transmission, the recovered population eventually begins to dwindle. Figure 7 shows the total number of new cases of malaria in proportion to the rate at which susceptible and infected people receive treatment. The graph indicates that the total number of new cases starts to decrease as the treatment rate rises. This indicates that increased treatment rates successfully lower the population's overall typhoid prevalence and burden.

CONCLUSION

This study a fractional-order mathematical model was developed to capture the complex dynamics of typhoid fever transmission, incorporating memory effects and nonlinear behavior often overlooked by traditional integer-order models. By employing the Adams–Bashforth method, we derived accurate numerical solutions that effectively describe the progression of the disease over time. The findings demonstrate that high contact and infection rates significantly facilitate the spread of typhoid fever, emphasizing the urgent need for improved sanitation, hygiene practices, and health education in vulnerable communities. Conversely, timely and effective treatment interventions were shown to drastically reduce infection rates, highlighting the vital role of accessible healthcare services, early diagnosis, and proper antibiotic use.The sensitivity analysis revealed that the most influential parameters in reducing disease burden include lowering the contact rate, enhancing treatment efficacy, and improving environmental conditions. These insights point to the need for integrated public health strategies that combine disease prevention, prompt medical care, and community-based hygiene education.

Furthermore, the study reinforces the pressing public health concern posed by typhoid fever, especially in regions with limited access to clean water and adequate healthcare infrastructure. The simulation results support a comprehensive approach to disease control—one that includes efficient management of contaminated sources, robust treatment protocols, and strengthened health systems

REFERENCE

Abah, E., Bolaji, B., Atokolo, W., Acheneje, G. O., Omede, B. I., Amos, J., & Omeje, D. (2025). Mathematical fractional model for the dynamics and control of diphtheria transmission. *International Journal of Mathematical Analysis and Modelling*, 7(2). https://tnsmb.org/journal/index.php/ijmam/article/view/182

Acheneje, G. O., Omale, D., Agbata, B. C., Atokolo, W., Shior, M. M., & Bolawarinwa, B. (2024). Approximate solution of the fractional order mathematical model on the transmission dynamics of the co-infection of COVID-19 and monkeypox using the Laplace–Adomian decomposition method. *IJMSS*, 12(3), 17–51.

Agbata, B. C., Obeng Denteh, W., Dervish, R., Kwabi, P. A., Aal Rkhais, H. A., Asante Mensa, F., Ezugorie, I. G., & Arivi, S. S. (2024). Mathematical modeling and analysis of monkeypox transmission dynamics with treatment and quarantine interventions. *DUJOPAS*, 10(4b), 78–96.

Agbata, B. C., Obeng-Denteh, W., Amoah-Mensah, J., Kwabi, P. A., Shior, M. M., Asante-Mensa, F., & Abraham, S. (2024). Numerical solution of fractional order model of measles disease with double dose vaccination. *Dutse Journal of Pure and Applied Sciences (DUJOPAS)*, 10(3b), 202–217. https://www.ajol.info/index.php/dujopas/article/view/281624

Agbata, B. C., Shior, M. M., Obeng-Denteh, W., Omotehinwa, T. O., Paul, R. V., Kwabi, P. A., & Asante-Mensa, F. (2023). A mathematical model of COVID-19 transmission dynamics with effects of awareness and vaccination program. *Journal of Ghana Science Association*, 21(2), 59–61. https://www.researchgate.net/publication/379485392 _

Ali, M., Zhang, X., & Wei, L. (2024). Fractional-order epidemiological model for tuberculosis with vaccination. *Scientific Reports*, 14(1), 73392. https://doi.org/10.1038/s41598-024-73392-x

Baskonus, H. M., & Bulut, H. (2015). On the numerical solutions of some fractional ordinary differential equations by the fractional Adams-Bashforth-Moulton method. *Open Mathematics*, 13, 1.

Bolaji, B., Onoja, T., Agbata, B. C., Omede, B. I., & Odionyenma, U. B. (2024). Dynamical analysis of HIV-TB co-infection transmission model in the presence of treatment for TB. *Bulletin of Biomathematics*, 2(1), 21–56. https://doi.org/10.59292/bulletinbiomath.2024002

Diethelm, K. (1999). The FracPECE subroutine for the numerical solution of differential equations of fractional order.

Gomez, F., Ramirez, J., & Castillo, D. (2023). Fractional-order SEIR model for COVID-19 dynamics in Argentina. *arXiv Preprint*, arXiv:2104.02853. https://arxiv.org/abs/2104.02853

Kim, J. H., Mogasale, V., Im, J., Ramani, E., Marks, F., & Ochiai, R. L. (2023). Typhoid fever: A comprehensive review of the literature. *Nature Reviews Disease Primers*, 9(1), Article 12. https://doi.org/10.1038/s41572-023-00480-z

Kumar, P., Kumar, S., Alkahtani, B. S. T., & Alzaid, S. S. (2024). A mathematical model for simulating the spread of infectious disease using the Caputo-Fabrizio fractional-order operator. *AIMS Mathematics*, 9(11), 30864–30897. https://doi.org/10.3934/math.20241490

Liu, B., Farid, S., Ullah, S., Altanji, M., Nawaz, R., & Teklu, S. W. (2023). Mathematical assessment of Monkeypox disease with the impact of vaccination using a fractional epidemiological modeling approach. *Scientific Reports*. http://dx.doi.org/10.1038/541598-023-40745-x

Odeh, J. O., Agbata, B. C., Ezeafulukwe, A. U., Madubueze, C. E., Acheneje, G. O., & Topman, N. N. (2024). A mathematical model for the control of chlamydia disease with treatment strategy. *Journal of Mathematical Acumen and Research*, 7(1), 45–60. https://www.researchgate.net/publication/381278254

Odeh, J. O., Agbata, B. C., Ezeafulukwe, A. U., Madubueze, C. E., Acheneje, G. O., & Topman, N. N. (2024). A mathematical model for the control of chlamydia disease with a treatment strategy. *Journal of Mathematical Analysis and Research*, 7(1), 1–20.

Odeh, J. O., Agbata, B. C., Tijani, K. A., & Madubueze, C. E. (2024). Optimal control strategies for the transmission dynamics of Zika virus: With the aid of Wolbachia-infected mosquitoes. *Numerical and Computational Methods in Sciences & Engineering*, 5(1), 1–25. https://doi.org/10.18576/ncmse/050101

Omowumi, F. L., Tunde, T. Y., & Afeez, A. (2024). On mathematical modeling of optimal control of typhoid fever with efficiency analysis. *Journal of the Nigerian Society of Physical Sciences*, 6(3), 2057. https://journal.nsps.org.ng/index.php/jnsps/article/view/2057

Patel, R., Sainani, P., Brar, M., Patel, R., Li, X., Drozd, J., Chishtie, F. A., Benterki, A., Scott, T. C., & Valluri, S. R. (2023). Modelling of COVID-19 using fractional differential equations. *arXiv Preprint*, arXiv:2307.16282. https://arxiv.org/abs/2307.16282

Sharma, P., Gupta, R., & Kumar, S. (2024). Integrating awareness and fractional-order delay differential equations in COVID-19 modeling. *BMC Medical Research Methodology*, 24(1), Article 2452. https://doi.org/10.1186/s12874-024-02452-7

Tadesse, G., Hassan, M., & Ahmed, R. (2024). Fractional-order modeling of COVID-19 and malaria co-infection. *Bulletin of Mathematical Biology*, 86(1), 15. https://doi.org/10.1007/s11538-024-0015

Tadesse, G., Tadesse, T., & Tadesse, M. (2024). Fractional-order epidemic model for measles infection. *Frontiers in Public Health*, 12, Article 1357131. https://doi.org/10.3389/fpubh.2024.1357131

Tadesse, G., Tadesse, T., & Tadesse, M. (2024). Prevalence of typhoid fever and its associated factors among febrile patients in Ethiopia: A cross-sectional study. *Frontiers in Public Health*, 12, Article 1357131. https://doi.org/10.3389/fpubh.2024.1357131

The Guardian. (2024, September 24). 'Drug-resistant typhoid is the final warning sign': Disease spreads in Pakistan as antibiotics fail. https://www.theguardian.com/global-development/2024/sep/24/drug-resistant-typhoid-disease-pakistan-antibiotics-superbugs-children

VandenDriessche, P., & Watmough, J. (2002). Reproduction numbers and sub-threshold endemic equilibria for compartmental models of disease transmission. *Mathematical Biosciences*, 180(1–2), 29–48.

World Health Organization. (2023). Typhoid. https://www.who.int/news-room/fact-sheets/detail/typhoid